Applied and Environmental Microbiology, Jan. 2011, p. 452–459 Vol. 77, No. 2
0099-2240/11/$12.00 doi:10.1128/AEM.00808-10

Switch between Life History Strategies Due to Changes in Glycolytic Enzyme Gene Dosage in *Saccharomyces cerevisiae*▽†

Shaoxiao Wang,[1]‡ Aymé Spor,[2]§ Thibault Nidelet,[3] Pierre Montalent,[3] Christine Dillmann,[2] Dominique de Vienne,[2] and Delphine Sicard[2]*

CNRS, UMR 0320/UMR 8120 Génétique Végétale, F-91190 Gif-sur-Yvette, France[1]; Université Paris-Sud, UMR 0320/UMR 8120 Génétique Végétale, F-91190 Gif-sur-Yvette, France[2]; and INRA, UMR 0320/UMR 8120 Génétique Végétale, F-91190 Gif-sur-Yvette, France[3]

Received 1 April 2010/Accepted 26 October 2010

Adaptation is the process whereby a population or species becomes better fitted to its habitat through modifications of various life history traits which can be positively or negatively correlated. The molecular factors underlying these covariations remain to be elucidated. Using *Saccharomyces cerevisiae* as a model system, we have investigated the effects on life history traits of varying the dosage of genes involved in the transformation of resources into energy. Changing gene dosage for each of three glycolytic enzyme genes (hexokinase 2, phosphoglucose isomerase, and fructose-1,6-bisphosphate aldolase) resulted in variation in enzyme activities, glucose consumption rate, and life history traits (growth rate, carrying capacity, and cell size). However, the range of effects depended on which enzyme was expressed differently. Most interestingly, these changes revealed a genetic trade-off between carrying capacity and cell size, supporting the discovery of two extreme life history strategies already described in yeast populations: the "ants," which have lower glycolytic gene dosage, take up glucose slowly, and have a small cell size but reach a high carrying capacity, and the "grasshoppers," which have higher glycolytic gene dosage, consume glucose more rapidly, and allocate it to a larger cell size but reach a lower carrying capacity. These results demonstrate antagonist pleiotropy for glycolytic genes and show that altered dosage of a single gene drives a switch between two life history strategies in yeast.

Adaptation to a given environment is characterized by an increase in fitness which is made possible by the existence of variation in life history traits such as age of maturity, growth rate, fecundity, and/or survival. Selection cannot maximize life history traits altogether because trade-offs limit the set of possible combinations of trait values. A trade-off occurs when an increase in fitness due to a change in one trait is opposed by a decrease in fitness due to a concomitant change in the second trait (51). The combinations of life history trait values that are selected for in a given population define life history strategies.

Phenotypic variation of life history strategies among species has been extensively described (51, 52, 60). However, predicting life history trait evolution still requires a better knowledge of the genetic bases of their variation and covariation (51, 60, 61). Quantitative trait loci (QTL) of life history traits have been mapped in many species (for a review, see references 25, 28, and 56), and variation in life history traits has been associated with variation in gene expression using a transcriptomics approach (reviewed in references 51 and 59). Spontaneous mutations in experimental evolution or mutagenesis experiments also allowed detection of genetic variation of life history traits (34, 35). However, these experiments did not separate *trans*-acting from *cis*-acting genetic effects, and the contribution of single genes versus epistasis effects remained difficult to evaluate. Furthermore, the origin of the genetic correlations, either linkage disequilibrium between separate loci or pleiotropy where a single gene has effects on two or more traits, could not be determined.

The budding yeast *Saccharomyces cerevisiae* has been shown recently to display genetic and plastic variations for life history traits (57, 58). Genetic correlations between traits revealed a continuum of life history strategies, ranging from the "grasshoppers," which consume glucose at a high rate and have a large cell size and a low carrying capacity, to the "ants," which consume glucose at a low rate and have a small cell size but reach a high carrying capacity. This study suggested that genes involved in glucose uptake were good candidates for studying the genetic bases of trade-offs between life history traits. More generally, glycolysis, which converts glucose into energy, appears as a central pathway for resource allocation to life history traits. A molecular signature of past selection has been detected for several glycolytic genes in a wide range of species (13, 45). However, in contrast, several mutant analyses have shown that the flux of the superpathway of glucose fermentation, including glycolysis, did not vary in response to changes in enzyme activities. For instance in *S. cerevisiae*, overexpressing separately eight glycolytic and alcoholic fermentation enzymes or overexpressing both phosphofructokinase and pyruvate ki-

* Corresponding author. Mailing address: Université Paris-Sud, UMR 0320/UMR 8120 Génétique Végétale, Ferme du Moulon, F-91190 Gif-sur-Yvette, France. Phone: 33 169332242. Fax: 33 169332340. E-mail: sicard@moulon.inra.fr.

‡ Present address: BRI F7-35, Department of Biochemistry and Molecular Biology, LSU Health Sciences Center—Shreveport, Shreveport, LA 71130.

§ Present address: Department of Microbiology, Cornell University, Ithaca, NY 14853.

▽ Published ahead of print on 12 November 2010.

† The authors have paid a fee to allow immediate free access to this article.

TABLE 1. Construction of yeast strains

Strain	Characteristics	Plasmid
BY4743	Wild-type diploid strain; *MAT***a**/*MAT*α *his3Δ1/his3Δ1 leu2Δ0/leu2Δ0 met15Δ0/MET15 LYS2/lys2Δ0 ura3Δ0/ura3Δ0*	
*hxk2*Δ/*hxk2*Δ strain	Double deletion mutant of *HXK2*; *MAT***a**/*MAT*α *his3Δ1/his3Δ1 leu2Δ0/ leu2Δ0 met15Δ0/MET15 LYS2/lys2Δ0 ura3Δ0/ura3Δ0 YGL253w::kanMX4/YGL253w::kanMX4*	Empty pCM190
*pgi1*Δ strain	One-copy deletion mutant of *PGI1*; *MAT***a**/*MAT*α *his3Δ1/his3Δ1 leu2Δ0/ leu2Δ0 met15Δ0/MET15 LYS2/lys2Δ0 ura3Δ0/ura3Δ0 YBR196c::kanMX4/YBR196c*	Empty pCM190
*fba1*Δ strain	One-copy deletion mutant of *FBA1*; *MAT***a**/*MAT*α *his3Δ1/his3Δ1 leu2Δ0/ leu2Δ0 met15Δ0/MET15 LYS2/lys2Δ0 ura3Δ0/ura3Δ0 YKL060c::kanMX4/YKL060c*	Empty pCM190
wt	Wild-type diploid strain; *MAT***a**/*MAT*α *his3Δ1/his3Δ1 leu2Δ0/leu2Δ0 met15*Δ0/*MET15 LYS2/lys2Δ0 ura3Δ0/ura3Δ0*	Empty pCM190
*hxk2*Δ/*hxk2*Δ *HKX2*^{over} strain	Double deletion mutant of *HXK2*; *MAT***a**/*MAT*α *his3Δ1/his3Δ1 leu2Δ0/ leu2Δ0 met15Δ0/MET15 LYS2/lys2Δ0 ura3Δ0/ura3Δ0 YGL253w::kanMX4/YGL253w::kanMX4*	pCM190-*HXK2*
*pgi1*Δ *PGI1*^{over} strain	One-copy deletion mutant of *PGI1*; *MAT***a**/*MAT*α *his3Δ1/his3Δ1 leu2Δ0/ leu2Δ0 met15Δ0/MET15 LYS2/lys2Δ0 ura3Δ0/ura3Δ0 YBR196c::kanMX4/YBR196c*	pCM190-*PGI1*
*fba1*Δ *FBA1*^{over} strain	One-copy deletion mutant of *FBA1*; *MAT***a**/*MAT*α *his3Δ1/his3Δ1 leu2Δ0/ leu2Δ0 met15Δ0/MET15 LYS2/lys2Δ0 ura3Δ0/ura3Δ0 YKL060c::kanMX4/YKL060c*	pCM190-*FBA1*
HXK2^{over} strain	Wild-type diploid strain; *MAT***a**/*MAT*α *his3Δ1/his3Δ1 leu2Δ0/leu2Δ0 met15Δ0/MET15 LYS2/lys2Δ0 ura3Δ0/ura3Δ0*	pCM190-*HXK2*
PGI1^{over} strain	Wild-type diploid strain; *MAT***a**/*MAT*α *his3Δ1/his3Δ1 leu2Δ0/leu2Δ0 met15Δ0/MET15 LYS2/lys2Δ0 ura3Δ0/ura3Δ0*	pCM190-*PGI1*
FBA1^{over} strain	Wild-type diploid strain; *MAT***a**/*MAT*α *his3Δ1/his3Δ1 leu2Δ0/leu2Δ0 met15Δ0/MET15 LYS2/lys2Δ0 ura3Δ0/ura3Δ0*	pCM190-*FBA1*

nase at the same time did not increase ethanol production (55). Increasing the expression of phosphoglucose isomerase in another yeast strain did not change the glucose flux either (4), and increasing the expression of phosphofructokinase did not affect glycolytic flux under anaerobic conditions (15). Altogether, these results suggest that glycolytic flux is at a plateau, where the variation of individual enzyme activities is buffered.

In spite of these data, the results of Spor et al. (57, 58) encouraged us to study whether changing glycolytic gene dosage could affect the glucose uptake rate and life history traits of *S. cerevisiae*. We focused on the three reversible reactions of the hexose part of the glycolytic pathway. This part includes the glucose-6-phosphate (G6P) branch point between glycolysis, the pentose phosphate (PP) pathway, trehalose biosynthesis, and the gluconeogenesis pathway. Glycolysis allows production of ATP necessary for cell growth in fermentation. The pentose phosphate pathway is a major cellular source of NADPH, which is used for reductive biosynthesis reactions and also generates precursors for the synthesis of nucleotides and amino acids. Trehalose and glycogen are carbohydrate storage molecules which can be reallocated to glycolysis or the PP pathway when needed. The G6P branch point enzymes can therefore play an important role in fitness, as shown in *Drosophila* (24). We constructed strains with four different gene dosages of these three glycolytic enzymes: the hexokinase 2 (one of the glucose phosphorylating enzymes), phosphoglucose isomerase, and fructose-1,6-bisphosphate aldolase (7). To do so, we used the wild-type (wt) diploid strain BY4743, deletion mutants of each gene, and multicopy plasmids containing each of these genes. In these strains, we analyzed the glucose consumption rate as well as cell size, growth rate, and carrying capacity. These three life history traits are expected to exhibit a genetic trade-off (57, 58). If their phenotypic covariation is the result of the variation in expression of one of our candidate genes and if the tested gene exhibits antagonistic pleiotropy, we expect to find that the variation of expression of a gene correlates positively with one life history trait but negatively with the other. If, in addition, the changes in gene dosage are associated with a change in glucose uptake rate, then pleiotropy is likely mediated by the different functions of the glycolytic pathway rather than by direct effects of a gene product on several traits.

MATERIALS AND METHODS

Construction of test strains. All the strains were constructed from the *S. cerevisiae* laboratory strain BY4743 (Table 1). The wild-type diploid strain, the one-copy deletion mutants of *PGI1* and *FBA1*, and both copies of a deletion mutant of *HXK2* were obtained from Euroscarf (Frankfurt, Germany). For one set of these strains, these four strains were transformed with the empty vector pCM190 (Euroscarf). These strains were denoted, respectively, the wt, *pgi1*Δ, *fba1*Δ, and *hxk2*Δ/*hxk2*Δ strains. For another set of these strains, they were transformed with the multicopy pCM190 vector containing one of the genes of interest. These strains are denoted the *PGI1*^{over}, *FBA1*^{over}, *HXK2*^{over}, *pgi1*Δ *PGI1*^{over}, *fba1*Δ *FBA1*^{over}, and *hxk2*Δ/*hxk2*Δ *HXK2*^{over} strains, where the superscript indicates overexpression of the gene in the vector. The pCM190 plasmid is an episomal yeast plasmid, which carries 2μm DNA sequence including the origin of replication (26). It also contains seven tetracycline-repressed expression promoters (*tetO* boxes) that were used to control expression of the genes of interest.

The construction of the overexpression plasmids started with amplification of the three genes of interest (*HXK2*, *PGI1*, and *FBA1*) from genomic DNA of the BY4743 wild-type strain. Three DNA fragments containing each gene flanked by BamHI and NotI sites were generated by PCR amplification using primers presented in Table 2. The PCR products were gel purified using a QiaQuick kit (Qiagen, Courtaboeuf, France), and the purified fragments were cloned into

TABLE 2. PCR primers used to amplify each of the three glycolytic genes, *HXK2*, *PGI1*, and *FBA1*

Name	Sequence (5′–3′)
5′ *FBA1*	GGATCCATGGGTGTTGAACAAATCTTAAAGAGAAAGAC
3′ *FBA1*	GCGGCCGCACCTTCAGAAGAAAAGAGCCGACCA
5′ *HXK2*	GGATCCATGGTTCATTTAGGTCCAAAAAAACCAC
3′ *HXK2*	GCGGCCGCAAGTTTAAGCACCGATGATACCAACG
5′ *PGI1*	GGATCCATGTCCAATAACTCATTCACTAACTTCAAACTG
3′ *PGI1*	GCGGCCGCTGCACATAATGTAGTTACTTGGACGCTG

pGEM-T (Promega, Charbonnières, France). After the sequences were confirmed, the three fragments were excised from pGEM-T by digestion with BamHI and NotI and again were gel purified using the QiaQuick kit. The resulting DNA fragments were ligated into the high-copy-number tetracycline-regulatable expression vector pCM190 that had been digested with BamHI and NotI (26). This resulted in the constructions of pCM190-*FBA1*, pCM190-*HXK2*, and pCM190-*PGI1*. The lithium acetate (LiAc) method was used to transform *S. cerevisiae* strains (27, 41). Because of the presence of a *URA3* marker on pCM190, the transformants were selected on synthetic complete medium lacking uracil (SC-URA). This medium consisted of 0.17% yeast nitrogen base without amino acids and without ammonium sulfate, 0.5% ammonium sulfate, 0.2% amino acid drop-out mix without uracil, and 2% glucose as a carbon source (53).

Yeast growth kinetics. Strains were streaked on SC-URA plates to get single colonies. For each strain, one colony was picked up and transferred into a 50-ml tube containing 20 ml of SC-URA liquid medium. After an overnight culture at 30°C, around 5×10^5 cells were transferred into a 50-ml tube containing 40 ml of fresh SC-URA liquid medium and incubated at 30°C with shaking. Every hour, 1 ml of culture was taken to measure the cellular density by spectrophotometry (optical density at 600 nm [OD_{600}]) and to estimate the extracellular glucose concentration as well as the enzyme activity. In addition, every 2 h, the number of CFU was counted by plating about 200 cells on two yeast-peptone-dextrose (YPD) agar plates so that we could estimate the relationship between the number of living cells (CFU) and cellular density (OD_{600}).

Enzyme assays. Total soluble protein extracts were prepared from cells harvested every hour during the growth assay. At each time point, cell pellets were resuspended in 30 μl of YeastBuster reagent (Novagen, Darmstadt, Germany) with 1 mM phenylmethylsulfonyl fluoride (PMSF) and incubated at room temperature for 20 min. After centrifugation at top speed for 10 min at 4°C, the supernatants were used as samples for enzyme assays. Bradford's method was used to determine the amount of total protein in at least 10-fold diluted crude cell extracts (8). All enzyme assays were carried out at 25°C, pH 7.5, in a final volume of 1 ml containing 50 mM PIPES (piperazine-*N*,*N*′-bis(2-ethanesulfonic acid) buffer, 100 mM potassium chloride, and 5 mM magnesium acetate (23).

The activity of total glucose-phosphorylating enzymes was determined by spectrophotometric measurement at 340 nm in an enzyme-coupled assay containing 0.4 mM NADP (Sigma, St. Louis, MO), 1.5 U of glucose-6-phosphate dehydrogenase (Sigma, St. Louis, MO), 1 mM ATP, 6 mM glucose, and cell extract. The enzyme activity measured was the sum of the activities of hexokinase isoenzyme 1 (Hxk1p), hexokinase isoenzyme 2 (Hxk2p), and glucokinase 1 (Glk1p). As we modified the expression level of only the *HXK2* gene, any variation in total glucose-phosphorylating activity is due to this enzyme.

Phosphoglucose isomerase (EC 5.3.1.9) activity was determined by spectrophotometric measurement at 340 nm in an enzyme-coupled assay containing 0.4 mM NADP, 1.8 U of glucose-6-phosphate dehydrogenase, 5 mM fructose-6-phosphate (Sigma, St. Louis, MO), and cell extract (36, 62).

Fructose-1,6-diphosphate aldolase (EC 4.1.2.13) activity was determined by spectrophotometric measurement of NADH oxidation at 340 nm in an enzyme-coupled assay containing 0.15 mM NADH (Sigma, St. Louis, MO), 4.3 U of glycerol-3-phosphate dehydrogenase (Sigma, St. Louis, MO), 50 U of triosephosphate isomerase (Sigma, St. Louis, MO), 6 mM glyceraldehyde-3-phosphate (Sigma, St. Louis, MO), and cell extract.

For each enzyme i ($i = 1, 2, 3$) and each level of expression j ($j = 1, 2, 3, 4$), we estimated the activity (A_{ij}) as μmole of substrate transformed per minute and per mg of total extracted cellular proteins ($\mu mole \cdot min^{-1} \cdot mg^{-1}$). The enzymatic activity was measured every hour over the growth assay and was found to be stable. The mean enzymatic activity was therefore calculated and used for statistical analyses. The enzymatic activity was calculated in three independent growth assays. Note that for figures, we show the mean enzymatic activity of each strain ij relative to the wild-type strain (A_{ij}/A_{wt}). Since the enzyme activity is the product of the catalytic constant (k_{cat}) and enzyme concentration (E_{ij}) and since k_{cat} is not modified by the change in gene copy number, the ratio A_{ij}/A_{wt} reflects the relative change in concentration.

Estimation of population size, growth rate, carrying capacity, cell size, and yield. During the growth assay, the optical density (OD_{600}) was measured every hour, and the number of CFU (population size N) was determined every 2 h. To estimate N at each time point, we analyzed the relationship between N and OD_{600} at the time points where we had both values using the following hyperbolic equation:

$$OD_{600} = \frac{a \times N}{b + N} \quad (1)$$

The parameters a and b were estimated for each strain and all repetitions. With the estimates of a and b, we calculated N from the OD_{600} at each time point, i.e., every hour, using the reciprocal relation, as follows: $N = (b \times OD_{600})/(a - OD_{600})$.

For each strain, the continuous change of population size was analyzed using the logistic model fitted to the estimated N values, i.e., every hour, as follows: $N_t = (N_0 \times K)/[N_0 + (K - N_0)e^{-rt}]$, where N_t is the population size at time t, N_0 is the initial population size, K is the carrying capacity (equivalent to the maximum population size), and r is the intrinsic growth rate (equivalent to the maximum rate of increase of the population). This model allowed us to estimate two fitness traits: the carrying capacity K and the intrinsic growth rate r. The growth rate at a specific time point (R_t) was calculated using the following relation: $R_t = (1/N_t)(dN_t/dt)$.

Cell size could be estimated indirectly using the OD_{600} value and the population size, N_t, because optical density depends on both cell size and the number of cells:

$$OD_{600_t} = CS_t \times N_t \quad (2)$$

where cell size (CS) is expressed in OD_{600} units per cell.

Using equation 1 and 2, cell size was deduced from the number of cells:

$$CS_t = \frac{OD_{600_t}}{N_t} = \frac{a}{b + N_t} \quad (3)$$

The yield was estimated as the product of cell size and carrying capacity divided by the amount of consumed glucose when the carrying capacity is reached.

Cell sizes were also independently measured in another experiment using a Beckman Coulter Counter Z2 (Fullerton, CA). The linear correlation between the cell sizes measured with the Coulter Counter and the estimated cell sizes from the OD_{600} values was highly significant ($P < 0.001$). The estimated cell sizes calculated at the time point when 25% of the glucose was consumed (T_{25}), when the other phenotypes were also quantified, were used for data analysis.

Glucose consumption rate. The glucose consumption rate, denoted J, was estimated by following the changes over time of the extracellular glucose concentration. The glucose consumed at time t was estimated by the difference between the initial extracellular concentration of glucose (20 g/liter) and the extracellular concentration of glucose at time t. Extracellular glucose concentration at time t was measured with an enzymatic kit (rBiopharm, Darmstadt, Germany) composed of two enzymes (hexokinase and glucose-6-phosphate dehydrogenase) which catalyze the following reactions:

$$\text{D–Glucose} + \text{ATP} \rightarrow \text{Glucose-6-Phosphate} + \text{ADP}$$

$$\text{Glucose-6-Phosphate} + \text{NADP}^+ \rightarrow \text{D–Gluconate-6-Phosphate} + \text{NADPH} + \text{H}^+ \quad (4)$$

The NADPH formed by this enzymatic reaction, measured by spectrophotometry at 365 nm, is stoichiometrically equal to the glucose present at the beginning of the reaction.

The change over time of the consumed glucose concentration (G_t) was fitted to a logistic model:

$$G_t = \frac{G_0 \times G_m}{G_0 + (G_m - G_0)e^{-v_m t}} \quad (5)$$

where G_t is the glucose concentration at time t, G_m is the initial and thus

TABLE 3. Analysis of variance testing the variation of quantitative traits in response to different expression levels of *HXK2*, *PGI1*, or *FBA1*

Parameter[a]	Value of the parameter for the indicated gene[b]								
	HXK2			*PGI1*			*FBA1*		
	df	MS	*F*	df	MS	*F*	df	MS	*F*
Log(A_i)									
Expression	3	20.97×10^{-2}	11.01**		24.87×10^{-2}	22.20***		11.25×10^{-2}	53.94***
Residuals	8	1.90×10^{-2}			1.12×10^{-2}			0.21×10^{-2}	
J_{T25}									
Expression	3	0.504	29.88***		0.354	14.25**		0.049	5.24*
Residuals	8	0.017			0.025			0.009	
R_{T25} (10^4)									
Expression	3	210.1	15.67***		12.19	0.61		10.15	0.60
Residuals	8	13.41			19.98			16.81	
Cell size (10^8)									
Expression	3	1.59	11.15**	3	0.94	20.73**	3	0.17	1,24
Block				2	0.58	12.71**	2	1.59	11,55**
Residuals	8	0.14		6	0.05		6	0.14	
K (10^{-6})									
Expression	3	350.41	29.79***	3	136.05	19.99***	3	57.62	53.24***
Block							2	6.24	5.76*
Residuals	8	11.76		8	6.805		6	1.08	
Yield (10^{-6})									
Expression	3	110.3	0.71	3	173.23	1.56	3	268.09	1.21
Block	2	838.49	5.43*	2	695.65	6.27*	2	1,548.44	6.98*
Residuals	6	154.46		6	110.88		6	221.88	

[a] A_i, activity of enzyme i; J_{T25}, specific glucose consumption rate; R_{T25}, growth rate; K, carrying capacity.
[b] df, degrees of freedom; MS, mean square. *, $P < 0.05$; **, $P < 0.01$; ***, $P < 0.001$.

maximum glucose concentration, v_m is the maximum rate of glucose consumption, and G_0 is the consumed glucose concentration at the beginning of the kinetics. It can be very small but not null.

The specific glucose consumption rate, i.e., the glucose consumption rate expressed in $g \cdot min^{-1} \cdot cell^{-1}$, was estimated as follows: $J_t = (1/N_t)(dG_t/dt)$.

Statistical analyses. Growth rate, glucose consumption rate, and cell size are changing over the population growth. To compare the tested strains, we had to choose a similar time point. We chose the beginning of the exponential phase, when 25% of the glucose is consumed. This also corresponded to the time when the specific glucose consumption rate (J_{T25}) is almost at its maximum.

Effect of changing gene expression. For each gene (*HXK2*, *PGI1*, and *FBA1*) and each phenotypic trait, the effect of the variation in gene expression was analyzed using the following linear model of analysis of variance: $Y_{jk} = \mu + \text{Block}_k + \text{Expression}_j + E_{jk}$, where Y_{jk} is the quantitative variable (A_i, J_{T25}, K, R_{T25}, CS_{T25}, or Yield), Block_k is the block effect ($k = 1, 2, 3$), and Expression_j is the gene expression effect ($j = 1, 2, 3, 4$). When we did not find any block effect, the block effect was deleted from the model. Mean differences between pairs of expression levels were assessed by contrast analysis. Due to heteroscedasticity of activity A_i, the variable was log transformed in order to meet the conditions of application for analysis of variance (ANOVA).

Relationship between fitness traits and glucose consumption rate. Over all the tested strains, i.e., including variation of expression for all enzymes, a regression analysis was performed to study the relationship between the specific glucose consumption rate at T_{25} (J_{T25}) and the fitness traits using the following model: $Y_{ijk} = \alpha J_{T25ijk} + \beta + E_{ijk}$, where Y_{ijk} is the phenotypic value of a fitness trait (R_{T25}, K, or CS), J_{T25ijk} is the specific glucose consumption rate of the strain having the jth level of expression ($j = 1, 2, 3, 4$) for enzyme i ($i = 1, 2, 3$) in block k ($k = 1, 2, 3$), α is the slope, β is the intercept, and E_{ijk} is the residual error.

Relationship between fitness traits. A Pearson correlation analysis over all tested strains, i.e., including variation of expression for all enzymes, was performed to study the pairwise relationships between the fitness traits.

RESULTS

For each enzyme (hexokinase isoenzyme 2, phosphoglucose isomerase, and fructose-1,6-bisphosphate aldolase), four strains with different levels of gene dosage were constructed (Table 1): a wild-type diploid strain containing an empty multicopy vector (wt), a strain with the target gene overexpressed in a multicopy plasmid (e.g., the *FBA1*^{over} strain), a hemizygous or homozygous deletion mutant containing an empty multicopy plasmid (e.g., the *fba1*Δ strain), and this deletion mutant with the target gene overexpressed in a multicopy plasmid (e.g., the *fba1*Δ *FBA1*^{over} strain).

As expected, changing gene dosage changed the enzymatic activity for all enzymes (Table 3 and Fig. 1). Hemizygous *pgi1*Δ and *fba1*Δ mutants had significantly lower activities ($P < 0.001$). In both cases, enzyme activity fell to about half of the wild-type activity. The *hxk2*Δ/*hxk2*Δ double deletion mutant also had a reduced level of glucose phosphorylating enzyme activity ($P = 0.016$). In this deletion mutant, the glucose phosphorylating activity was provided only by the two other phosphorylating enzymes, hexokinase isoenzyme 1 (Hxk1p) and glucokinase 1 (Glk1p) (5, 12, 66).

Increasing gene expression in the wild-type strain by adding the multicopy plasmid resulted in all cases in an increase in enzyme activity compared to that of the wild-type strain (P 0.031 for the *HXK2* strain, $P = 0.013$ for the *PGI1* strain, and $P = 0.004$ for the *FBA1* strain) (Fig. 1). Similarly, increasing

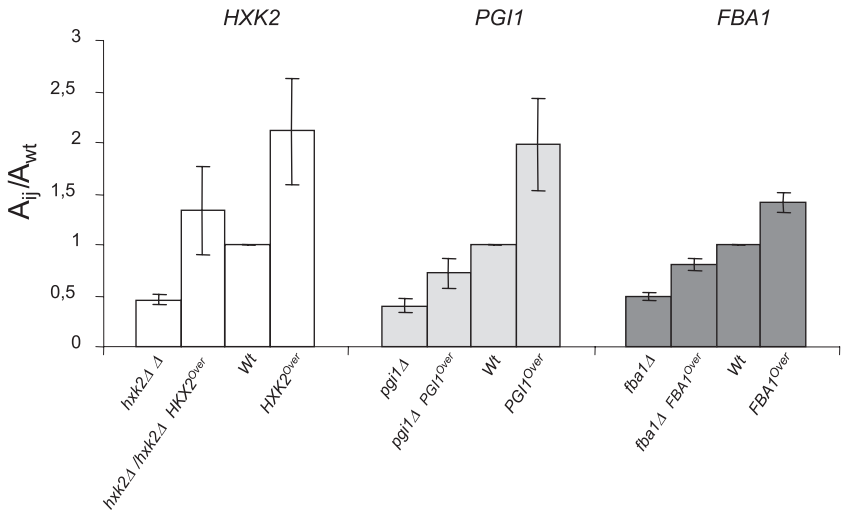

FIG. 1. Mean activity of glucose-phosphorylating enzymes (white bars), phosphoglucose isomerase (gray bars), and fructose-1,6-bisphosphate aldolase (dark gray bars) in expression mutants relative to the wild-type (wt) strain (A_{ij}/A_{wt}). The symbol Δ indicates deletions of one (*pgi*Δ and *fba*Δ) or two (*hxk2*Δ/*hxk2*Δ) genomic copies. Overexpression of a gene in the multicopy pCM190 vector is indicated by a superscript (over).

gene expression in deletion mutants by adding the multicopy plasmid increased the mean activity for all enzymes ($P = 0.006$ for the *HXK2* strain, $P = 0.021$ for the *PGI1* strain, and $P < 0.001$ for the *FBA1* strain) (Fig. 1).

Changing the dosage of any of the three glycolytic genes led to glucose consumption rate and life history trait variation but did not change significantly the yield, i.e., the biomass produced per gram of glucose (Table 3). The magnitude of the phenotypic effect was gene dependent.

The double deletion of *HXK2* had the most noticeable effects. It led to a 2-fold decrease of the mean glucose consumption rate relative to that of the wild-type ($P < 0.001$). Deletion of *HXK2* also led to a decreased growth rate and a decreased cell size but increased carrying capacity. Interestingly, increasing expression of *HXK2* did not change the glucose consumption rate but seemed to be costly since it led to a decreased growth rate ($P = 0.08$ for the difference between the wt and *HXK2*^{over} strains and $P = 0.01$ for the difference between the *hxk2*Δ/*hxk2*Δ *HXK2*^{over} and *HXK2*^{over} strains) and decreased carrying capacity ($P = 0.009$ for the difference between the *hxk2*Δ/*hxk2*Δ *HXK2*^{over} and *HXK2*^{over} strains).

Deleting one of the two copies of *PGI1* had no effect on either the glucose consumption rate or life history traits. In contrast, increasing *PGI1* copy number in the wild-type strain led to a significantly increased glucose consumption rate ($P < 0.001$). This was associated with an increased cell size ($P < 0.001$) and decreased carrying capacity ($P < 0.001$) but had no effect on growth rate, which was robust in spite of any changes in *PGI1* expression.

Deleting one copy of *FBA1* in the wild-type diploid strain had no significant effect on either the glucose consumption rate or the fitness traits. In contrast, increasing expression of *FBA1* improved the glucose consumption rate of the wild-type strain ($P = 0.046$) and of the hemizygous deletion mutant ($P < 0.001$). This is associated with a significantly decreased carrying capacity ($P < 0.001$ for the wt versus the *FBA1*^{over} strain and $P = 0.007$ for the *fba1*Δ strain versus the *fba1*Δ *FBA1*^{over} strain). No significant variation in growth rate and cell size was detected when changing *FBA1* expression.

With four levels of gene dosage for three genes and three replicates, we got a range of 36 values of the glucose consumption rate. The relationship between the glucose consumption rate and each of the life history traits was analyzed (Fig. 2).

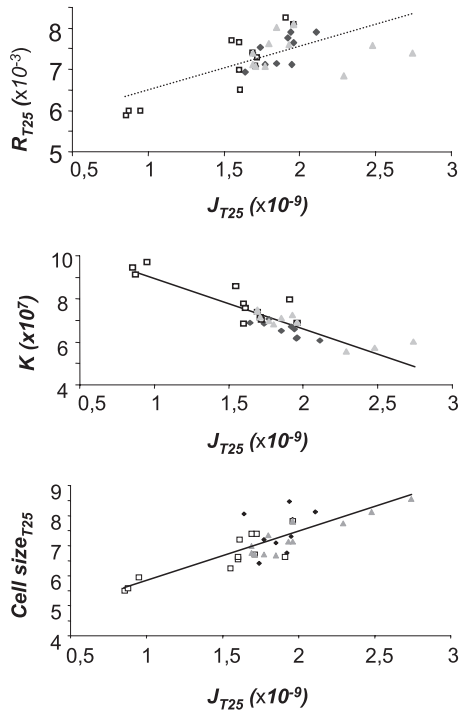

FIG. 2. Relationships between the glucose consumption rate (J_{T25}) and growth rate (R_{T25}), carrying capacity, or cell size. Each point is obtained from a replicate of a transformed strain. Open squares, *HXK2*-transformed strains; gray triangles, *PGI1*-transformed strains; black diamonds, *FBA1*-transformed strains.

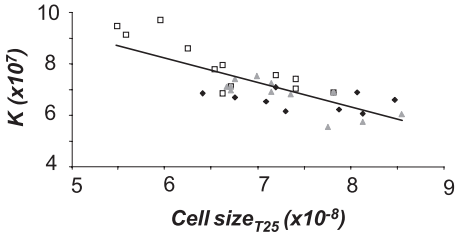

FIG. 3. Relationship between the carrying capacity (K) and cell size. The symbols are the same as those described in the legend of Fig. 2.

Since the yield did not vary significantly between strains, we did not analyze its correlation with other traits.

A positive correlation between the glucose consumption rate and growth rate was observed ($R^2 = 0.42$; $P < 0.001$). This correlation was mainly due to the *HXK2* deletion mutant since the correlation was no more significant when the three corresponding data points were excluded from the analysis. A positive correlation between the glucose consumption rate and cell size was found ($R^2 = 0.64$; $P < 0.001$) and remained significant without the *HXK2* deletion mutant points ($R^2 = 0.44$; $P < 0.001$). Finally, a negative correlation between the glucose consumption rate and carrying capacity was detected ($R^2 = 0.78$; $P < 0.001$), even when the *HXK2* deletion mutant points were excluded ($R^2 = 0.55$; $P < 0.001$).

A negative correlation between the carrying capacity and cell size was detected over the 12 strains ($R^2 = 0.62$; $P < 0.001$) (Fig. 3). A negative correlation was found between the growth rate and carrying capacity ($R^2 = 0.25$; $P = 0.002$), and a positive one was found between the growth rate and cell size ($R^2 = 0.26$; $P = 0.002$), but these correlations were not detected when the mutants lacking *HXK2* were excluded.

DISCUSSION

We showed that changing the activity of an enzyme by changing its gene dosage led to a change of glucose uptake rate along an ascending saturation curve. This type of relationship is consistent with the metabolic control analysis (MCA) framework (29, 31, 62) and has been observed in several biological systems, both *in vitro* by reconstructing metabolic pathways (23) and *in vivo* in plants (33), animals (54), and microbes (14, 32).

Increasing activity of Pgi1p or Fba1p 1.5- to 2-fold led to a significant increase in the glucose uptake rate. These results challenge the common idea that yeast glycolytic flux is at a plateau and cannot be increased by increasing the activity of glycolytic enzymes. They contrast with the conclusion of a classical paper that showed that increasing expression of several glycolytic genes did not modify ethanol production (55). Discrepancy with our results might be due to the fact that we have analyzed the glucose uptake rate rather than the fermentation rate. Alternatively, the results can simply reveal genetic background and/or environment effects, as observed in a number of other eukaryotic and prokaryotic organisms (2, 3, 20, 63). Therefore, glycolytic flux might be improved by altering glycolytic gene dosage in yeast.

We showed that changing gene dosage of glycolytic genes led to a quantitative change of the three life history traits (growth rate, carrying capacity, and cell size). However, growth rate was less affected than carrying capacity and cell size (Table 3). It did not vary significantly in response to a change of *PGI1* and *FBA1* gene dosage, which can be explained by the fact that glucose can be used for storage and not for growth and proliferation.

Changing the *HXK2* gene dosage resulted in variation of the growth rate, which is consistent with the predominant role played by Hxk2p in glucose phosphorylation during fermentative growth (5, 66). In addition, Hxk2p interacts with a catabolic repressor complex (1, 21, 39, 40). Therefore, its deletion activates the expression of many genes, which can be costly for the cell (17, 49).

Changing the dosage of *HXK2* or *PGI1* led to a significant change in cell size. The genetic components of cell architecture, including cell size, have been previously studied using QTL mapping and systematic deletion approaches (38, 42, 43). The genetic bases of morphological parameters appear to be complex, with evidence of both epistasis and transgressive segregation, and the QTLs and genes identified by the two approaches did not match. Here, we showed that cell size is linked to glycolytic genes. Although an earlier report related cell size to growth rate (65), more recent studies revealed that, in continuous culture under respiro-fermentative growth conditions, cell size increases when glucose metabolism shifts to ethanol production independently of the specific growth rate (47, 48). Ethanol may act as a quorum-sensing signal, leading to an increase in cell size (30). Our data provide genetic evidence supporting the link between cell size and glycolytic flux under fermentative growth conditions, independent of the growth rate.

To our knowledge the genetic control of carrying capacity has not been previously studied. The carrying capacity is classically defined as the maximum population size that a given environment can support given finite resources (16). It reflects the ability of a population to survive and/or colonize other environments. It should not be confounded with yield, which depends on both the carrying capacity and cell size. In ecology, when it is expressed in mathematical models, K is often considered a fixed parameter, the value of which depends only on resource availability. Thus, the within-species genetic differences are often assumed to be negligible. We used the resource consumption rate to show that this parameter depends on the genotype of individuals. Its phenotypic mean value varied in response to a change of expression of any of the three investigated glycolytic genes. This result highlights the need for including genetic components of carrying capacity in population dynamics modeling.

Cell size and carrying capacity were negatively correlated when the gene dosage of any of the three enzymes was changed. Only a few studies have analyzed the genetic bases of life history trait correlations, and so far only in rare cases has single-gene pleiotropy been demonstrated. The development of microarray technology has allowed the exploration of molecular mechanisms of trade-offs and the identification of genes that affect life history traits in opposite ways. In *Drosophila melanogaster*, a shift between energy metabolism and protein biosynthesis, regulated by the RAS signaling pathway, could explain the trade-off between larval survival and adult

size (6). In whitefish, the differences between two life history strategies can be associated with upregulation of genes involved in energy metabolism, lipid metabolism, iron homeostasis, and detoxification and with downregulation of genes involved in protein synthesis, cell cycle, and cell growth (59). However, in most cases, the identification of pleiotropic genes involved in genetic correlations between life history traits is hampered by the fact that genetic correlation can also be due to linkage disequilibrium or to the influence of a third unmeasured trait (11, 50).

The few studies investigating pleiotropic effects of spontaneous mutations are mainly restricted to a few life history traits in two model species, *D. melanogaster* (22, 35, 67) and *Arabidopsis thaliana* (9, 37). In *Drosophila*, the general consensus from these studies seems to be that mutations affecting life history traits tend to produce intermediate-to-high positive correlations (22), with little evidence of genetic trade-offs generated by antagonistic pleiotropy. In *Arabidopsis*, McKay et al. (37) provided good evidence to suggest that shared QTL underlying flowering time and water use efficiency represent truly pleiotropic genes. Similarly, Camara et al. (9, 10) detected pleiotropic loci in *Arabidopsis*, notably for flowering time and number of rosette leaves. However, examples of pleiotropic genes accounting for life history trade-offs remain sparse.

We showed that several genes of a single pathway may display pleiotropy for life history traits. We had previously observed a negative correlation between carrying capacity and cell size by studying a collection of yeast strains (57, 58) and had defined two extreme life history strategies, those of the ants and the grasshoppers described above. Here, we showed that changing the expression of a single glycolytic gene allows a shift from one strategy to the other. The switch between life history strategies occurred under fermentation conditions and did not result in significant yield variation. Therefore, the two adaptation strategies did not reflect the well-known metabolic trade-off between fermentation and respiration. It seems, rather, that the two strategies are related to the allocation of glucose to either internal cellular storage or energy for increased population size. One can see the grasshopper strategy as a selfish one where the individuals allocate resources to their own use and survival and the ant strategy as a cooperative one where resources are allocated to the whole population. Our results suggest that glycolytic genes would be directly involved in such a social strategy. Trade-offs between life history traits have been hypothesized to arise as a consequence of metabolic competition for resources (6) or pleiotropic effects independent from resource allocation (18, 59). We showed that both explanations may be linked: genes involved in resource uptake may display pleiotropy for life history traits.

Further developments of this work will concern the significance of the results for real environmental niches to determine if strains isolated from various niches and having different life history strategies show the three genes upregulated and/or present at different copy numbers. Even though variation in gene copy numbers in yeast evolution is largely documented (19, 46, 64), we did not find in the yeast sequencing genome database any evidence for copy number variation for HXK2, PGI1, and FBA1 in the nine strains previously characterized as typical of ants and grasshoppers (54). So the variation of these enzymes, if any, would reside in the levels of expression. Experimental evolution of several strains in different environments would be another way to study the genetic bases of life history strategy variation. Such a work is in progress in our laboratory. Convergence toward the ant or grasshopper strategy, depending upon the environment, was observed. The results of genome sequencing of ancestral and evolved strains are being analyzed to identify the selected mutations. With the diversity of genetic backgrounds and the pervasiveness of epistasis (44), several molecular scenarios are expected.

In summary, our findings give the first example of pleiotropic genes affecting both fitness traits and social strategies through quantitative variation of metabolic rate of a single pathway. Although other genes are probably involved in differences between ant and grasshopper life history strategies, our results allow a better understanding of the metabolic constraints on fitness trait variation.

ACKNOWLEDGMENTS

We thank Adrienne Ressayre and Jean-Marie François for scientific discussions and critical reading of the manuscript. We are grateful to Kelly Tatchell and Lucy Robinson for revising the language.

This work was supported by the French Agence Nationale de la Recherche (ANR Project ADAPTALEVURE number NT05-4_45721). The postdoctoral fellowships of Shaoxiao Wang and Thibault Nidelet were supported by CNRS.

REFERENCES

1. **Ahuatzi, D., P. Herrero, T. de la Cera, and F. Moreno.** 2004. The glucose-regulated nuclear localization of hexokinase 2 in *Saccharomyces cerevisiae* is Mig1-dependent. J. Biol. Chem. **279:**14440–14446.
2. **Bakker, B. M., et al.** 1999. Contribution of glucose transport to the control of the glycolytic flux in *Trypanosoma brucei*. Proc. Natl. Acad. Sci. U. S. A. **96:**10098–10103.
3. **Beatty, C. H., R. M. Bocek, and M. K. Young.** 1975. Glycolytic control mechanisms in myometrium from pregnant rhesus monkeys. Biol. Reprod. **12:**408–414.
4. **Benevolensky, S. V., D. Clifton, and D. G. Fraenkel.** 1994. The effect of increased phosphoglucose isomerase on glucose metabolism in *Saccharomyces cerevisiae*. J. Biol. Chem. **269:**4878–4882.
5. **Bianconi, M. L.** 2003. Calorimetric determination of thermodynamic parameters of reaction reveals different enthalpic compensations of the yeast hexokinase isozymes. J. Biol. Chem. **278:**18709–18713.
6. **Bochdanovits, Z., and G. de Jong.** 2004. Antagonistic pleiotropy for life-history traits at the gene expression level. Proc. Biol. Sci. **271**(Suppl. 3)**:**S75–S78.
7. **Brachmann, C. B., et al.** 1998. Designer deletion strains derived from *Saccharomyces cerevisiae* S288C: a useful set of strains and plasmids for PCR-mediated gene disruption and other applications. Yeast **14:**115–132.
8. **Bradford, M. M.** 1976. A rapid and sensitive method for the quantitation of microgram quantities of protein utilizing the principle of protein-dye binding. Anal. Biochem. **72:**248–254.
9. **Camara, M. D., C. A. Ancell, and M. Pigliucci.** 2000. Induced mutations: a novel tool to study phenotypic integration and evolutionary constraints in *Arabidopsis thaliana*. Evol. Ecol. Res. **2:**1009–1029.
10. **Camara, M. D., and M. Pigliucci.** 1999. Mutational contributions to genetic variance/covariance matrices: an experimental approach using induced mutations in *Arabidopsis thaliana*. Evolution **53:**1692–1703.
11. **Clark, A. G.** 1987. Variation in Y chromosome segregation in natural populations of *Drosophila melanogaster*. Genetics **115:**143–151.
12. **Clifton, D., R. B. Walsh, and D. G. Fraenkel.** 1993. Functional studies of yeast glucokinase. J. Bacteriol. **175:**3289–3294.
13. **Conant, G. C., and K. H. Wolfe.** 2007. Increased glycolytic flux as an outcome of whole-genome duplication in yeast. Mol. Syst. Biol. **3:**129.
14. **Cronwright, G. R., J. M. Rohwer, and B. A. Prior.** 2002. Metabolic control analysis of glycerol synthesis in *Saccharomyces cerevisiae*. Appl. Environ. Microbiol. **68:**4448–4456.
15. **Davies, S. E., and K. M. Brindle.** 1992. Effects of overexpression of phosphofructokinase on glycolysis in the yeast *Saccharomyces cerevisiae*. Biochemistry **31:**4729–4735.
16. **del Monte-Luna, P.** 2004. The carrying capacity of ecosystems. Glob. Ecol. Biogeogr. **13:**485–495.
17. **Diderich, J. A., L. M. Raamsdonk, A. L. Kruckeberg, J. A. Berden, and K. Van Dam.** 2001. Physiological properties of *Saccharomyces cerevisiae* from

which hexokinase II has been deleted. Appl. Environ. Microbiol. **67:**1587–1593.
18. **Drnevich, J. M., M. M. Reedy, E. A. Ruedi, S. Rodriguez-Zas, and K. A. Hughes.** 2004. Quantitative evolutionary genomics: differential gene expression and male reproductive success in *Drosophila melanogaster*. Proc. Biol. Sci. **271:**2267–2273.
19. **Dunham, M. J., et al.** 2002. Characteristic genome rearrangements in experimental evolution of *Saccharomyces cerevisiae*. Proc. Natl. Acad. Sci. U. S. A. **99:**16144–16149.
20. **Emmerling, M., J. E. Bailey, and U. Sauer.** 1999. Glucose catabolism of *Escherichia coli* strains with increased activity and altered regulation of key glycolytic enzymes. Metab. Eng. **1:**117–127.
21. **Entian, K. D.** 1980. Genetic and biochemical evidence for hexokinase PII as a key enzyme involved in carbon catabolite repression in yeast. Mol. Gen. Genet. **178:**633–637.
22. **Fernandez, J., and C. Lopez-Fanjul.** 1996. Spontaneous mutational variances and covariances for fitness-related traits in *Drosophila melanogaster*. Genetics **143:**829–837.
23. **Fievet, J. B., C. Dillmann, G. Curien, and D. de Vienne.** 2006. Simplified modelling of metabolic pathways for flux prediction and optimization: lessons from an in vitro reconstruction of the upper part of glycolysis. Biochem. J. **396:**317–326.
24. **Flowers, J. M., et al.** 2007. Adaptive evolution of metabolic pathways in *Drosophila*. Mol. Biol. Evol. **24:**1347–1354.
25. **Gardner, K. M., and R. G. Latta.** 2007. Shared quantitative trait loci underlying the genetic correlation between continuous traits. Mol. Ecol. **16:**4195–4209.
26. **Gari, E., L. Piedrafita, M. Aldea, and E. Herrero.** 1997. A set of vectors with a tetracycline-regulatable promoter system for modulated gene expression in *Saccharomyces cerevisiae*. Yeast **13:**837–848.
27. **Gietz, R. D., and R. A. Woods.** 2002. Transformation of yeast by lithium acetate/single-stranded carrier DNA/polyethylene glycol method. Methods Enzymol. **350:**87–96.
28. **Gutteling, E. W., et al.** 2007. Environmental influence on the genetic correlations between life-history traits in *Caenorhabditis elegans*. Heredity **98:**206–213.
29. **Heinrich, R., and T. A. Rapoport.** 1973. Linear theory of enzymatic chains; its application for the analysis of the crossover theorem and of the glycolysis of human erythrocytes. Acta Biol. Med. Ger. **31:**479–494.
30. **Kacmar, J., A. Gilbert, J. Cockrell, and F. Srienc.** 2006. The cytostat: a new way to study cell physiology in a precisely defined environment. J. Biotechnol. **126:**163–172.
31. **Kacser, H., and J. A. Burns.** 1973. The control of flux. Symp. Soc. Exp. Biol. **27:**65–104.
32. **Koebmann, B., C. Solem, and P. R. Jensen.** 2005. Control analysis as a tool to understand the formation of the *las* operon in *Lactococcus lactis*. FEBS J. **272:**2292–2303.
33. **Lauerer, M., et al.** 1993. Decreased ribulose-1,5-bisphosphate carboxylase-oxygenase in transgenic tobacco transformed with "antisense" *rbcS*. Planta **190:**332–345.
34. **Lenski, R. E.** 2004. Phenotypic and genomic evolution during a 20,000-generation experiment with the bacterium *Escherichia coli*. Plant Breed. Rev. **24:**225–265.
35. **Lynch, M.** 1985. Spontaneous mutations for life-history characters in an obligate parthenogen. Evolution **39:**804–818.
36. **Maitra, P. K., and Z. Lobo.** 1971. A kinetic study of glycolytic enzyme synthesis in yeast. J. Biol. Chem. **246:**475–488.
37. **McKay, J. K., J. H. Richards, and T. Mitchell-Olds.** 2003. Genetics of drought adaptation in *Arabidopsis thaliana*: I. Pleiotropy contributes to genetic correlations among ecological traits. Mol. Ecol. **12:**1137–1151.
38. **Millar, J. B.** 2002. A genomic approach to studying cell-size homeostasis in yeast. Genome Biol. **3:**REVIEWS1028. http://genomebiology.com/content/3/10/REVIEWS1028.
39. **Moreno, F., D. Ahuatzi, A. Riera, C. A. Palomino, and P. Herrero.** 2005. Glucose sensing through the Hxk2-dependent signalling pathway. Biochem. Soc. Trans. **33:**265–268.
40. **Moreno, F., and P. Herrero.** 2002. The hexokinase 2-dependent glucose signal transduction pathway of *Saccharomyces cerevisiae*. FEMS Microbiol. Rev. **26:**83–90.
41. **Mount, R. C., B. E. Jordan, and C. Hadfield.** 1996. Transformation of lithium-treated yeast cells and the selection of auxotrophic and dominant markers. Methods Mol. Biol. **53:**139–145.
42. **Nogami, S., Y. Ohya, and G. Yvert.** 2007. Genetic complexity and quantitative trait loci mapping of yeast morphological traits. PLoS Genet. **3:**e31.
43. **Ohya, Y., et al.** 2005. High-dimensional and large-scale phenotyping of yeast mutants. Proc. Natl. Acad. Sci. U. S. A. **102:**19015–19020.
44. **Phillips, P. C.** 2008. Epistasis—the essential role of gene interactions in the structure and evolution of genetic systems. Nat. Rev. Genet. **9:**855–867.
45. **Pierce, V. A., and D. L. Crawford.** 1997. Phylogenetic analysis of glycolytic enzyme expression. Science **276:**256–259.
46. **Piskur, J., E. Rozpedowska, S. Polakova, A. Merico, and C. Compagno.** 2006. How did *Saccharomyces* evolve to become a good brewer? Trends Genet. **22:**183–186.
47. **Porro, D., L. Brambilla, and L. Alberghina.** 2003. Glucose metabolism and cell size in continuous cultures of *Saccharomyces cerevisiae*. FEMS Microbiol. Lett. **229:**165–171.
48. **Porro, D., M. Vai, M. Vanoni, L. Alberghina, and C. Hatzis.** 2009. Analysis and modeling of growing budding yeast populations at the single cell level. Cytometry A **75:**114–120.
49. **Raamsdonk, L. M., et al.** 2001. Co-consumption of sugars or ethanol and glucose in a *Saccharomyces cerevisiae* strain deleted in the HXK2 gene. Yeast **18:**1023–1033.
50. **Roff, D. A.** 2002. Life history evolution. Sinauer Associates Inc., Sunderland, MA.
51. **Roff, D. A., and D. J. Fairbairn.** 2007. The evolution of trade-offs: where are we? J. Evol. Biol. **20:**433–447.
52. **Roff, D. A., S. Mostowy, and D. J. Fairbairn.** 2002. The evolution of trade-offs: testing predictions on response to selection and environmental variation. Evolution **56:**84–95.
53. **Rose, M. D., F. Winston, and P. Hieter.** 1990. Methods in yeast genetics: a laboratory course manual. Cold Spring Harbor Laboratory Press, Cold Spring Harbor, NY.
54. **Salter, M., R. G. Knowles, and C. I. Pogson.** 1986. Quantification of the importance of individual steps in the control of aromatic amino acid metabolism. Biochem. J. **234:**635–647.
55. **Schaaff, I., J. Heinisch, and F. K. Zimmermann.** 1989. Overproduction of glycolytic enzymes in yeast. Yeast **5:**285–290.
56. **Sgro, C. M., and A. A. Hoffmann.** 2004. Genetic correlations, tradeoffs and environmental variation. Heredity **93:**241–248.
57. **Spor, A., S. Wang, C. Dillmann, D. de Vienne, and D. Sicard.** 2008. "Ant" and "grasshopper" life-history strategies in *Saccharomyces cerevisiae*. PLoS One **3:**e1579.
58. **Spor, A., et al.** 2009. Niche-driven evolution of metabolic and life-history strategies in natural and domesticated populations of *Saccharomyces cerevisiae*. BMC Evol. Biol. **9:**296.
59. **St-Cyr, J., N. Derome, and L. Bernatchez.** 2008. The transcriptomics of life-history trade-offs in whitefish species pairs (*Coregonus* sp.). Mol. Ecol. **17:**1850–1870.
60. **Stearns, S. C.** 1982. Components of fitness. Science **218:**463–464.
61. **Stearns, S. C., and P. Magwene.** 2003. The naturalist in a world of genomics. Am. Nat. **161:**171–180.
62. **Teusink, B., et al.** 2000. Can yeast glycolysis be understood in terms of in vitro kinetics of the constituent enzymes? Testing biochemistry. Eur. J. Biochem. **267:**5313–5329.
63. **Thomas, S., P. J. Mooney, M. M. Burrell, and D. A. Fell.** 1997. Metabolic control analysis of glycolysis in tuber tissue of potato (*Solanum tuberosum*): explanation for the low control coefficient of phosphofructokinase over respiratory flux. Biochem. J. **322:**119–127.
64. **Thomson, J. M., et al.** 2005. Resurrecting ancestral alcohol dehydrogenases from yeast. Nat. Genet. **37:**630–635.
65. **Tyson, C. B., P. G. Lord, and A. E. Wheals.** 1979. Dependency of size of *Saccharomyces cerevisiae* cells on growth rate. J. Bacteriol. **138:**92–98.
66. **Walsh, R. B., G. Kawasaki, and D. G. Fraenkel.** 1983. Cloning of genes that complement yeast hexokinase and glucokinase mutants. J. Bacteriol. **154:**1002–1004.
67. **Yoshimaru, H., and T. Mukai.** 1985. Relationships between the polygenes affecting the rate of development and viability in *Drosophila melanogaster*. Jpn. J. Genet. **60:**307–334.